Earthquakes and Structures, *Vol. 14, No. 6 (2018) 599-614*
DOI: https://doi.org/10.12989/eas.2018.14.6.599

Earthquake performance assessment of low and mid-rise buildings: Emphasis on URM buildings in Albania

Huseyin Bilgin*[1] and Ergys Huta[2]

[1]*Department of Civil Engineering, EPOKA University, Rruga Tirane, Km 12, 1032, Tirana, Albania*
[2]*Albania Draht, Mucaj, Vore, Tirana, Albania*

(Received July 26, 2016, Revised April 29, 2018, Accepted May 8, 2018)

Abstract. This study focuses on the earthquake performance of two URM buildings having typical architectural configurations common for residential use constructed per pre-modern code in Albania. Both buildings are unreinforced clay brick masonry structures constructed in 1960 and 1984, respectively. The first building is a three-storey unreinforced one with masonry walls. The second one is confined masonry rising on five floors. Mechanical characteristics of masonry walls were determined based on experimental tests conducted according to ASTM C67-09 regulations. A global numerical model of the buildings was built, and masonry material was simulated as nonlinear. Pushover analyses are carried out to obtain capacity curves. Displacement demands were calculated according to Eurocode 8 and FEMA440 guidelines. Causes of building failures in recent earthquakes were examined using the results of this study. The results of the study showed that the URM building displays higher displacement and shear force demands that can be directly related to damage or collapse. On the other hand, the confined one exhibits relatively higher seismic resistance by indicating moderate damage. Moreover, effects of demand estimation approaches on performance assessment of URM buildings were compared. Deficiencies and possible solutions to improve the capacity of such buildings were discussed.

Keywords: capacity assessment; capacity spectrum; confined masonry; seismic performance; unreinforced masonry structures

1. Introduction

Following the destructive earthquakes in recent decades, the seismic performance assessment of existing buildings continues to be one of the priorities of structural engineers in many earthquake prone countries. A considerable number of the older URM and RC buildings are in moderate to severe seismic areas of the world with various levels of seismic hazard (Inel *et al*. 2008, Korkmaz 2009, Yilmaz *et al*. 2013, Bilgin 2013, Preciado *et al*. 2018). In order to recognize the most critical regions and mitigate the future earthquake consequences, a proper assessment of seismic risk in existing buildings is an important step. To achieve this goal, seismic risk assessment with reliable mathematical models of these structures are needed. In recent years, several models characterized by different levels of complexity have been developed and proposed for masonry structures and aimed at different analyses types in literature (Lourenço 1996, Lagomarsino *et al*. 2003, Bilgin 2007, Chen *et al*. 2008, Calderini and Lagomarsino 2008).

Recent earthquakes around the world have highlighted the vulnerability of the masonry structures since most of them were built with no detailed guidelines or regulations. Many of them were severely affected due to poor quality of construction, workmanship, aging as well as the lack of maintenance (Decanni *et al*. 2004, Klinger 2006, Kaplan *et al*. 2010, Bilgin and Korini 2012) and left thousands of people homeless. They provide shelter for millions of people and their goods (Bilgin and Huta 2016). Thus, destruction of masonry structures can seriously endanger people's life. In such situations, the intervention to enhance a higher seismic performance becomes very crucial. The first step to complete this task is to understand the real response and adequately assess the actual seismic performance of masonry structures.

Safety evaluation of buildings should be based on both qualitative (as gathering knowledge about the structure, observation, survey and description of the damage pattern, etc.) and quantitative (as in-situ and laboratory experimental tests, mathematical, etc.) methods that consider the effect of the phenomena on structural response (Foraboschi and Vanin 2013a). Any assessment of structural safety is seriously influenced by the uncertainty attached to data (actions, deformations, resistance, etc.), laws, models, assumptions, etc. used in the study, and by the difficulty of representing real phenomena in a precise way (Lourenço 2010, Mendes and Lourenço 2010).

In Albania, masonry was widely used for buildings intended for residential and public services during the communist period (1944-1990) due to its cost effectiveness with the template designs developed by the governmental authorities (Bilgin and Korini 2012). Thus, they represent a high percentage in residential stock and the typical typology of the Albania corresponds to URM construction. There are standard URM buildings all over the country for residential

*Corresponding author, Associate Professor
E-mail: hbilgin@epoka.edu.al

ISSN: 2092-7614 (Print), 2092-7622 (Online)

purposes, 2 to 5 stories with different template plans. Most of the existing residential masonry buildings in the country, like in many other European countries were designed considering earlier codes KTP-9 (1978), KTP-N2, (1989), Bilgin (2015) when seismic loads were not required, or the design was to reduce the level of seismic loads. Moreover, past studies and reconnaissance team reports (Kaplan *et al*. 2010, Bilgin and Korini 2012, Preciado *et al*. 2014), Preciado *et al*. 2015, Preciado *et al*. 2016) suggest that URM construction is vulnerable under seismic actions. Therefore, this type of construction is prone to earthquake failures.

This study aims at evaluating the seismic performance of the typical low and mid-rise existing masonry residential buildings constructed per pre-modern seismic code from Albanian construction practice. In order to reflect the properties of low and mid-rise existing URM buildings, two residential buildings having 3- and 5-storey with template

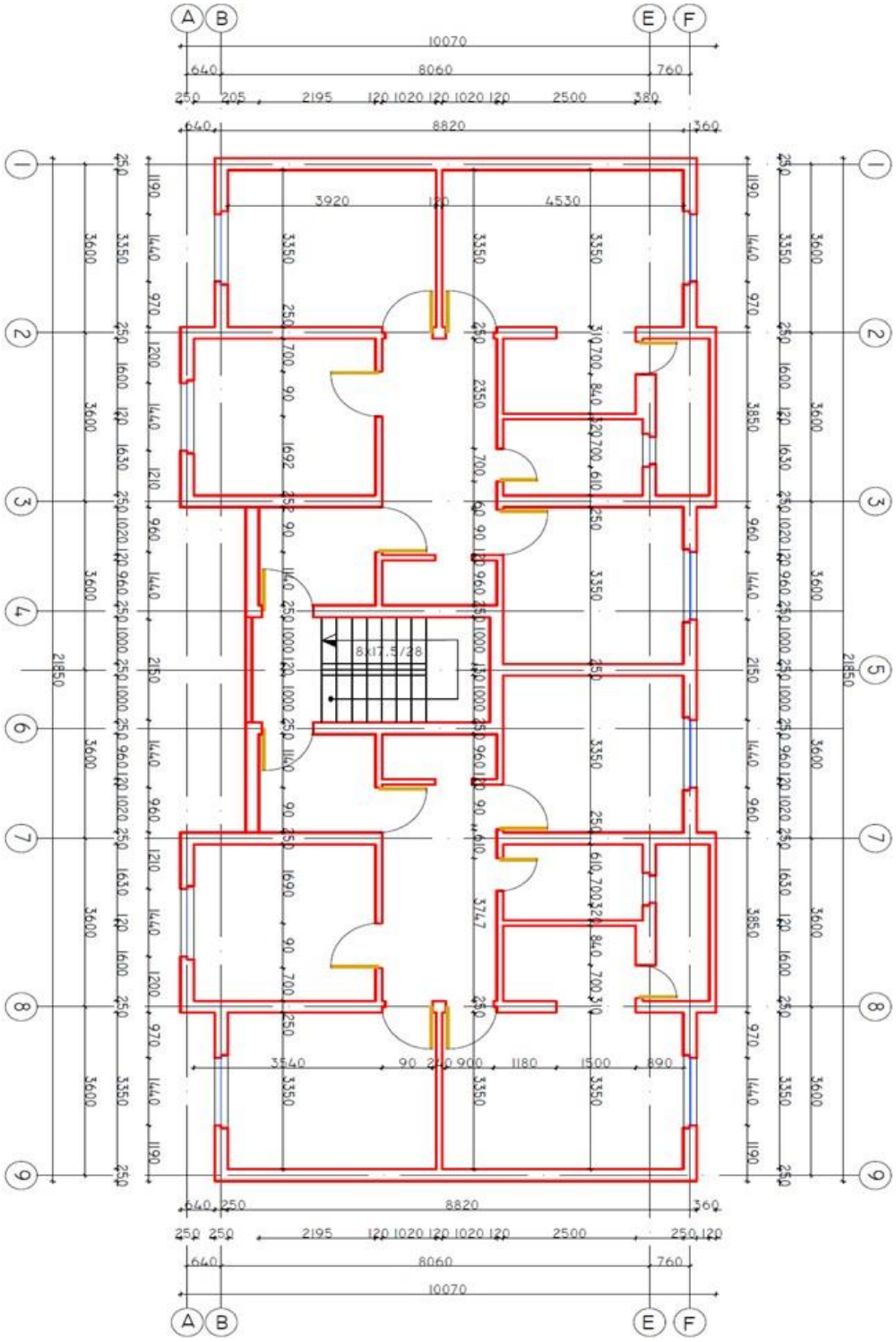

Fig. 1 Typical plan view of the 3-storey URM building, units in mm

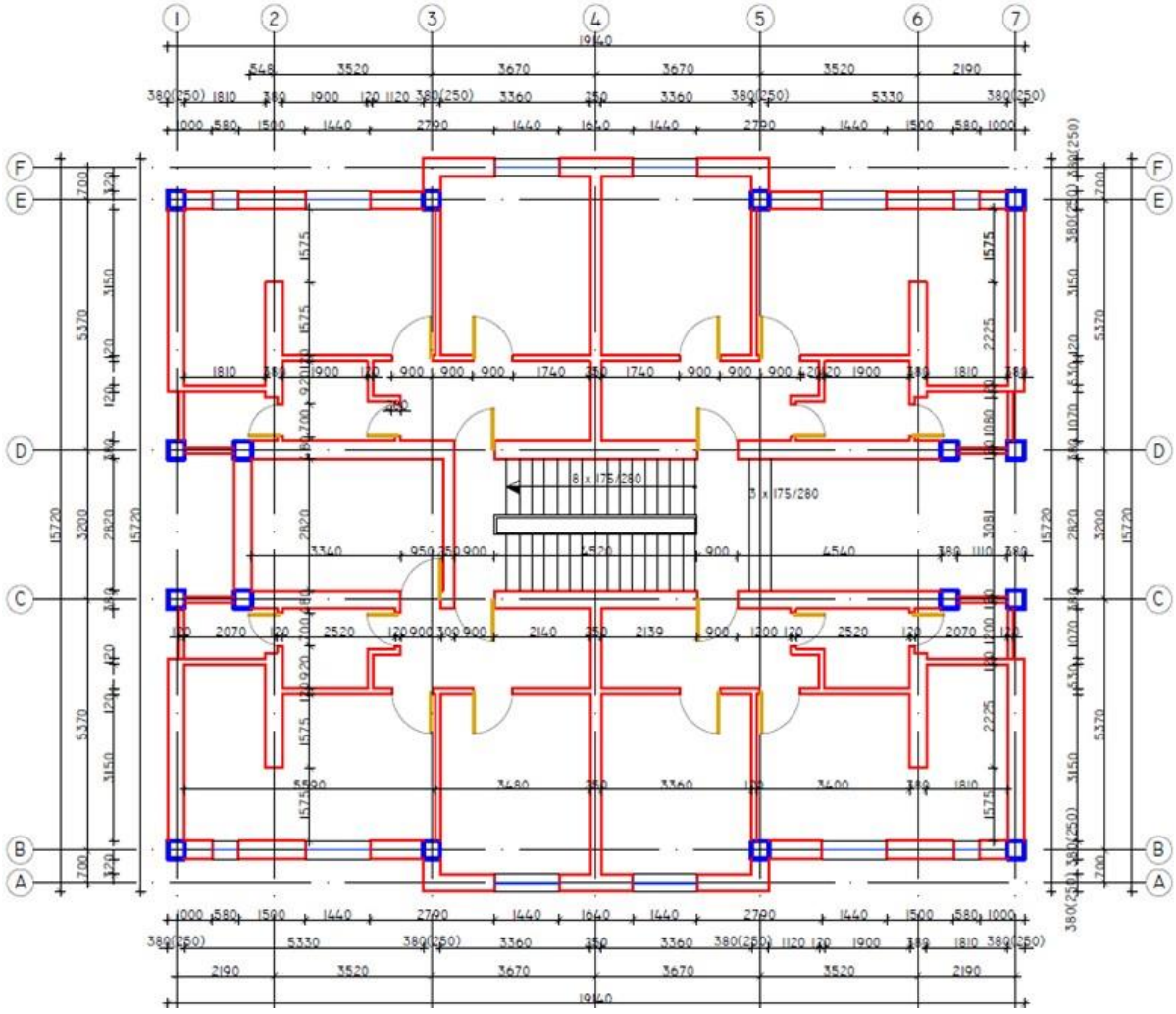

Fig. 2 Typical plan view of the 5-storey URM building, units in mm

designs constructed in accordance with Albanian Code KTP-9 (1978) were selected and modelled by using the DIANA v 9.6 (2014). Structural features such as member dimensions, material types and loading conditions of the buildings were determined from their architectural and structural designs projects and field investigations. Mechanical characteristics were determined experimentally and adopted for nonlinear analysis. During the capacity evaluation, damage limit states were determined by using two different criteria given in literature (Calvi 1999, Lagomarsino and Penna 2003). Nonlinear force-deformation response of the buildings was determined by pushover analysis. It is worth to mention that pushover analysis was deployed in each direction under two lateral load patterns.

Demand predictions are also as important as capacity estimation for seismic performance assessment. In literature, there are several approaches for the calculation of the seismic demand in terms of displacement. Damping based FEMA 440 (2004) and *R*-μ-*T* based EN1998-1 (2004) estimations were adopted in many international codes and guidelines. In this study, both estimation methods EN1998-1 and FEMA 440 were used for seismic demand estimations.

2. Description of the selected buildings

The objects of the investigation are two masonry buildings constructed between the 1960's and 1980's in Tirana, Albania. This period corresponds to the communist era (1944-1990) which explains the fact that these buildings were built according to template projects approved by the government construction institutions due to its low cost. In other words, standard procedures were followed to design and build such buildings. Masonry was commonly used for public and governmental buildings as a low-cost construction method for that time. Today these buildings are still in use and the main functions are mostly for residential purposes. Hence, a considerable number of buildings have the same template designs in different parts of Albania Korini (2012).

Typical building typology for essential facilities in Albania is template designs of low and mid-rise URM buildings. These structures are composed of two main components, namely load bearing walls and roof diaphragms. The walls are stiff with openings and the diagrams are usually constructed by RC slabs. For the scope of the study, a field and archive survey were carried out in Tirana city to select the most common template designs

among residential buildings. Two benchmark URM buildings were selected as typical existing low and mid-rise buildings in the region. The first case study building presented in Fig. 1 represents the common typology of low-rise buildings in the region. Similar buildings were constructed during the communist period making a stock of residential masonry buildings built according to KTP-N.2-60 regulations Huta (2015). This type has three stories with brick walls of 250 mm for the load bearing walls and 120 mm for other partition walls. It has 21.85 m×10.70 m dimensions in plan with a regular storey height of 2.8 m. Solid bricks with 250 mm×125 mm×60 mm dimensions connected with cement mortar were used to build the masonry walls. In order to achieve a better distribution of the loads, perimeter RC beams were used to create a better connection between slabs and load bearing walls.

The second typology represents a 5- storey confined masonry built in 1984 according to KTP-N.2-78 regulations KTP-9 (1978). It has 19.14 m×15.72 m plan dimensions with a regular storey height of 2.8 m (Fig. 2). The load bearing walls were made with masonry walls that can be classified in facade with a thickness of 380 mm and inner masonry walls 250 mm thick. The thickness of outer load bearing walls of first two stories have 380 mm and the remaining three stories are 250 mm. Calcium silicate solid bricks with 250 mm×125 mm×65 mm dimensions connected with cement mortar were used to build the masonry walls. Partition walls are 120 mm thick made of calcium silicate solid bricks and cement mortar. The slabs are pre-stressed RC joists with hollow concrete with a thickness of 220 mm and a flat roof. The columns have 380 mm×380 mm dimensions and they were made of reinforced concrete. Beam width varies from 250 mm to 380 mm depending on the load bearing walls on which they were constructed.

3. Material properties

For the mathematical modeling and the analysis of the selected buildings, material properties determined from site investigations and experimental tests were taken into consideration. As mentioned formerly, many of the buildings intended for residential purposes have similar construction practices supervised by the governmental authorities. In order to truly represent the strength and structural integrity of the buildings, mechanical characteristics were obtained from the experimental tests with destructive methods. It is worthy to mention that five full masonry units on load bearing walls (250 mm×125 mm×60 mm) should be selected to test according to ASTM C67-09 (2008) guidelines. Randomly selected specimens in each building were identified to meet the minimum requirements of standards for the number of tests (Figs. 3-4).

Then, the samples were tested to determine the compressive strength of the solid brick units (Fig. 5). The aforementioned method for determining the compressive strength was applied to the both buildings and results were presented in Table 1.

The average compressive strength of the samples for 3-storey building was found to be as f_b=18.06 MPa. The minimum compressive strength among the five samples taken in consideration is $f_{b\min}$=17.22 MPa. On the other hand, the average compressive strength of the samples is for 5-storey building is f_b=16.52 MPa. The minimum compressive strength among the five samples taken in consideration is $f_{b\min}$=14.67 MPa.

For the determination of the compressive strength of mortars, samples of mortar were taken from the areas where the connection between solid brick units and mortar has failed. Due to the irregular shape of the samples, capping is required to be done according to ASTM C 109/C 109M - 02 regulations ASTM (2008). Test procedures were shown in Fig. 6. Using this technique, the average compressive strength of mortars was found to be 3.88 MPa and ~10 MPa for 3- and 5- storey buildings, respectively.

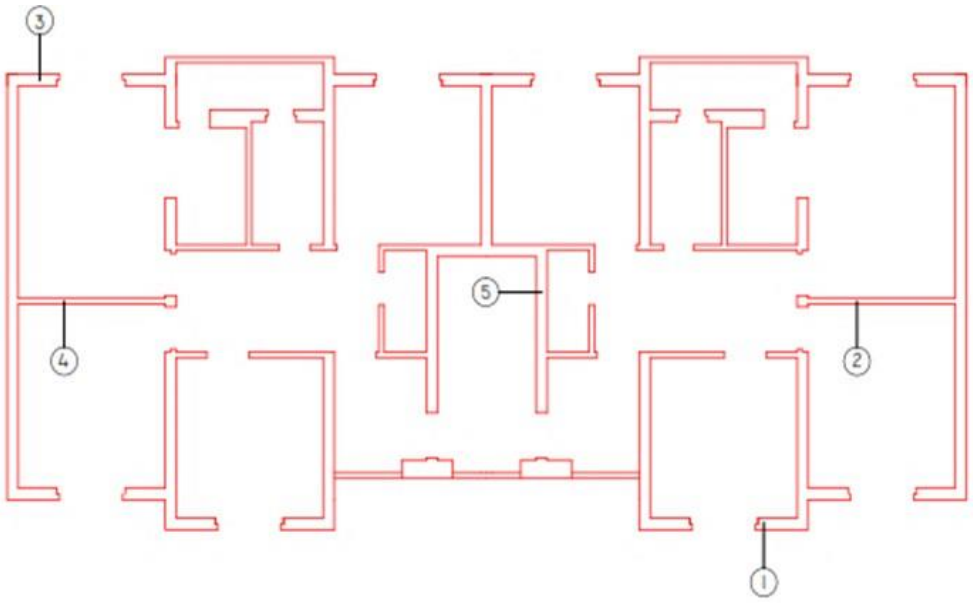

Fig. 3 Location of the samples for the determination of the weight and compressive strength of solid bricks (URM)

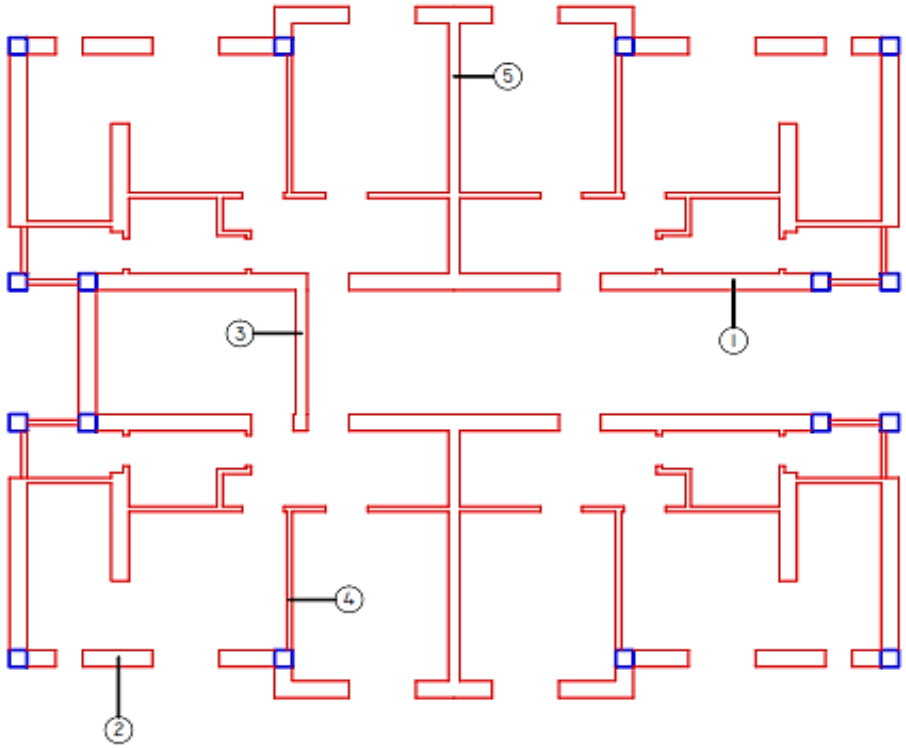

Fig. 4 Location of the samples for the determination of the weight and compressive strength of solid bricks (Confined Masonry Building)

(a)

(b)

Fig. 5 (a) Sample during testing, (b) Sample after testing

(a)

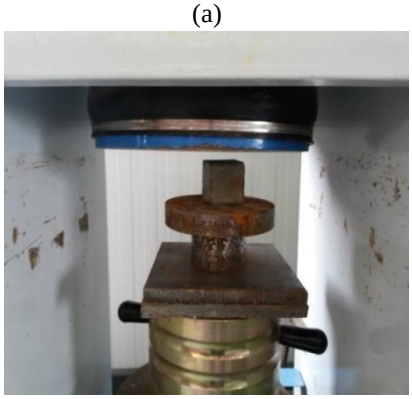

(b)

Fig. 6 (a) Sample before testing, (b) Sample during testing

In the case when experimental data is not sufficient, several equations are proposed by different codes and guidelines to calculate the compressive strength of the masonry walls. In this study, Eurocode 6 CEN (2005) guideless were followed as given below:

$$f_k = K * f_b^{0.70} * f_m^{0.30} \text{ (MPa)} \quad (1)$$

where:

Table 1 Masonry wall data used as input for analytical modeling

Building Type	Compressive strength f_k (N/mm^2)	Compressive fracture energy G_{fc} (N/mm^2)	Tensile strength f_t (N/mm^2)	Tensile fracture energy G_t (N/mm)	Shear strength f_t (N/mm^2) as per EC 6	E (N/mm^2) as per EC 6	Poisson ratio v
3- storey	4.35	6.96	0.2175	0.1	0.21	4350	0.2
5- storey	5.47	8.752	0.2735	0.1	0.31	5470	0.2

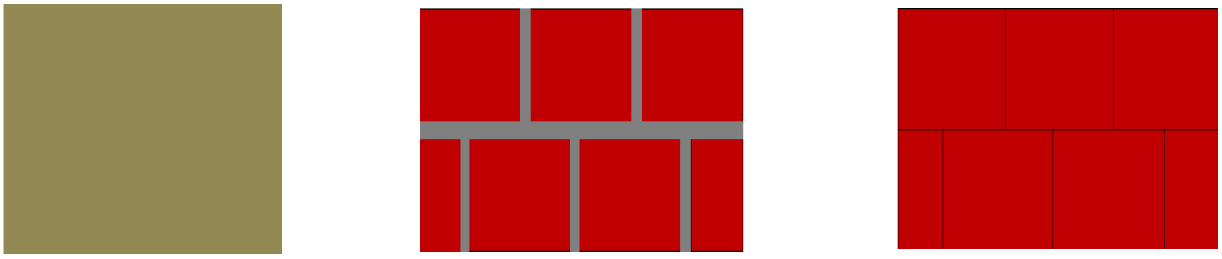

(a) (b) (c)

Fig. 7 Modeling strategies: (a) Macro-modeling, (b) Micro-modeling, (c) Meso-modeling

f_b: Normalized mean compressive strength of masonry units,

f_m: Mean compressive strength of mortar

K: Empirical coefficient that depends on the classification of masonry units.

Tensile strength is usually taken as 5% of the compressive strength (Lourenço *et al*. 2005). To obtain the normalized compressive strength of masonry units, the mean compressive strength of the tested units is multiplied by the δ factor which is given in Eurocode 6 (CEN 2005). If there is no experimental data, Eurocode 6 recommends taking the modulus of elasticity equal to E=1000f_k [MPa]. For the calculation of fracture energy, Eq. (2) is used (Lourenço *et al*. 2005).

$$G_f = 0.025 * (2*f_t)^{0.7} \text{ (MPa)} \quad (2)$$

where:

G_f: Tensile fracture energy,

f_t: Tensile strength.

Following the Eurocode 6 guidelines together with the relevant material characteristics obtained from experimental tests were used to calculate the required input data for mathematical modeling of the buildings (Table 1). Details of the calculations can be found in the relevant literature (Huta 2015).

4. Modeling approach

Modeling masonry structures is not an easy task due to the nonlinear behaviour of masonry and lack of experimental data regarding the inherent characteristics of masonry structural elements. In order to get the required data regarding the geometry and structural details, in situ investigations have been conducted. Original designs were obtained from the archives of official authorities. Laboratory tests were done to determine the mechanical and physical properties of the materials. Member sizes and reinforcements were used to model the selected buildings for nonlinear analysis. All members were modelled as given in the template designs without any simplifications; such as grouping members or rounding-off similar amounts. Masonry is a heterogeneous material composed of masonry bricks and mortar of which mechanical characteristics depend upon the inherent properties of its constituents. Its behaviour under different loadings may be very complex. In order to model the response of masonry, numerous assumptions and analytical models are proposed in literature (Lagomarsino *et al*. 2007, Calderini and Lagomarsino 2008, Farshchi *et al*. 2009, Lourenço 2010);

- Macro-modeling (Wang *et al*. 2012) where units and mortar are smeared out. This technique is based on equivalent properties and the principle of homogenization (Fig. 7(a)). In this approach, the brick masonry which is made from two different materials of the mortar and clay bricks had been replaced by an equivalent homogenous material. The macro-models are based on the use of constitutive laws for the masonry material; i.e., the stress-strain relationships adopted for the structural analysis are derived by performing tests on masonry, without distinguishing the bricks and the mortar behavior. The meso-level and the macro-level modeling technique are unable to model the local failure modes (unlike the micro-modeling technique),

- Micro-modeling (Augenti and Paris 2011), which is the most detailed type of modeling. Properties of both unit and mortar were used and crack patterns were defined prior to the analysis (Fig. 7(b)). Micro level models consider the units and the mortar joints distinctly, characterized by different constitutive laws; thus, the structural analysis is achieved considering each constituent of the masonry material. The inherent mechanical properties that characterize the models adopted for the brick units and the mortar joints are obtained through experimental tests conducted on the single material components,

- Meso-modeling Cagnan (2012), or it can be also named as simplified micro-modeling. This technique offers a balanced approach between the two other techniques (Fig. 7(c)). In meso-level modeling; expanded components are characterized by continuum elements. The response of the mortar joints and the unit/mortar interface are concentrated into discontinuum elements. In this modeling approach, the

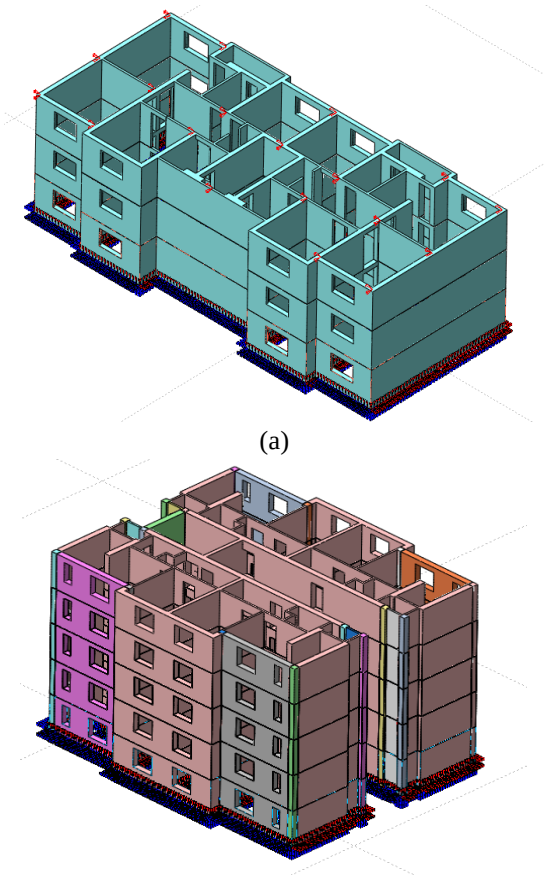

(a) (b)

Fig. 8 3D view of the unreinforced masonry building models (DIANA v.9.6) (a) 3-storey; (b) 5-storey

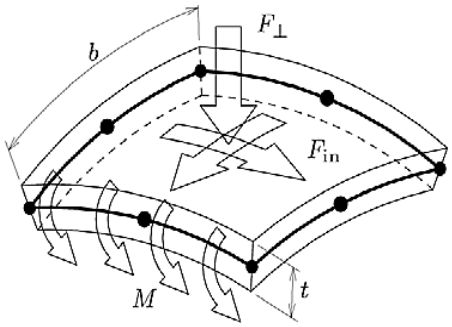

Fig. 9 Curved shell element used for modeling (DIANA 2014)

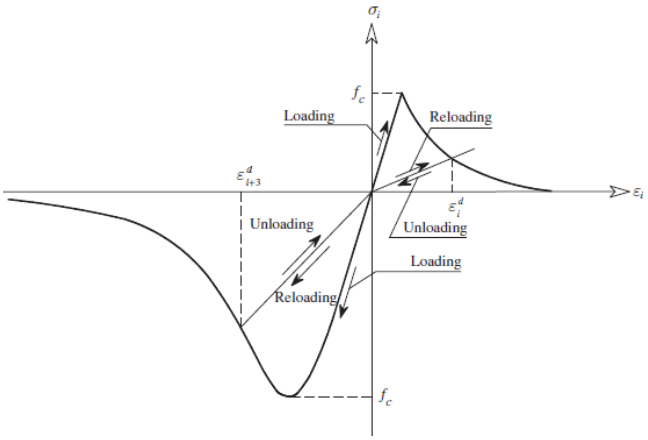

Fig. 10 Adopted hysteretic behavior of masonry (Mendes and Lourenço 2010)

units are expanded to retain the initial geometry of the masonry assemblage. Due to the assumption of the zero width of mortar joints, the elastic properties of the expanded brick units are adjusted to yield the Young modulus of the considered masonry. In the stack merged brick masonry prism, the bricks are assumed as a series of chain connection of the components yield the uniform stress distributions both in the mortar and brick unit.

Each of these techniques requires the adoption of different constitutive models. Due to the complexity of the two case study buildings, several assumptions on the material properties and the necessity of having high performance computers to process the nonlinear analyses, macro-modeling technique was considered. Nonlinear static analyses were conducted by DIANA v 9.6 software that is a multi-purpose finite element program dedicated for the linear and nonlinear analysis of masonry structures DIANA (2014). A 3-D model of each building typology was created in DIANA to carry out pushover analysis (Fig. 8(a)-(b)).

Walls were modelled as nonlinear-layered curved shell (quadrilateral element CQ40S type) elements (Fig. 9). This type of element is characterized by eight nodes and five degrees of freedom for each node (40 degrees of freedom per element). For these elements, in plane Gauss integration scheme was adopted with 3×3 integration points on the sides (Zienkiewicz *et al*. 2005). In order to capture the nonlinear behaviour through the thickness, five points were selected according to Simpson rule. As iteration method, the regular Newton-Rapson method was selected with arc-length control. Shear deformation is considered according to Mindlin-Reisner theory and the normal stress component to the surface element is equal to zero DIANA (2014).

Mechanical nonlinear behaviour of the masonry wall was defined through the total strain fixed crack model detailed in DIANA v 9.6 software DIANA (2014). In this approach, the cracks are fixed in the direction of the principal strain vectors kept unchanged during the loading process.

For the hysteretic response of masonry, parabolic stress-strain relation for compression was chosen based on Hill-type yield criterion (Fig. 10). A compressive strength of 4.35 N/mm^2 and 5.47 /mm^2 were adopted for 3- and 5-storey buildings, respectively. For the tension path, based on Rankine-type yield criterion was introduced by an exponential tension-softening diagram, adopting a tensile strength of 0.2175 N/mm^2 and 0.2735 N/mm^2 for 3- and 5-storey buildings, respectively.

Post-cracked response was defined by considering the retention factor of its linear behaviour which decreases its shear capacity as follows:

$$G^{cr} = \beta G \tag{3}$$

where;

β: retention factor ($0<\beta\leq 1$),

G: Shear modulus of the uncracked material

The default value for retention factor (β=0.01) was used

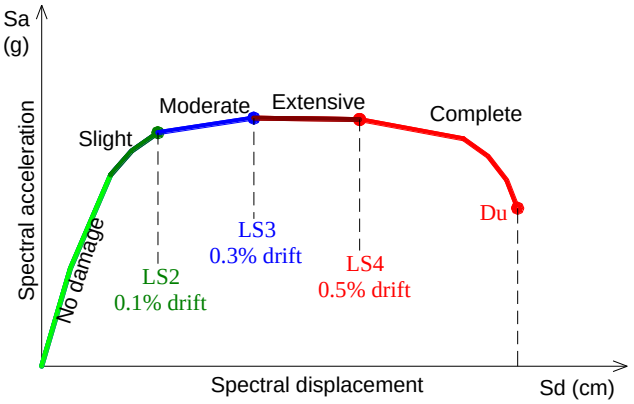

Fig. 11 Performance levels on pushover curve for masonry

meaning that the shear strength of the material will be reduced to one percent of the original shear strength when cracks develop. Crack bandwidth "*h*" was considered as follows Eq. (4)

$$h = A^{1/2} \tag{4}$$

where;

A: total in-plane area of the 2-D element,

The walls are the load bearing elements, while the floors are considered as stiffening elements, on which the lateral effects are distributed between the connected walls. In this study, out-of-plane response of walls and local flexural response of floors have been neglected since they are considered as negligible with respect to the global building response dominated by their in-plane response. Perimeter beams (ring beams) in masonry prevents out-of-plane failure and provides the development of global structural behaviour governed by in-plane response of walls. This fact was also observed in previous shaking table tests (Benedetti *et al*. 1998).

4.1 Definition of damage limit states

Damage limit states are quantitative definition of performance levels by a convenient damage indicator capable of representing the seismic performance with appropriate damage thresholds. A quantitative measure of building response can be estimated with drift values as displacements and deformation quantities. Selection of these drift thresholds are influenced by several factors including building typology, boundary conditions, level of axial loading as well as construction details. In literature, several damage limit states have been proposed based on the results of pushover analyses. Calvi (1999), Lagomarsino and Penna (2003) proposed different thresholds of the spectral displacement for discrete damage states based on the bilinear representation of the capacity spectrum. Since there are neither experimental test results nor available values calibrated with observed earthquake damages for the case study buildings, both limit states were employed to make a comparative performance assessment of the considered template designs. Schematic capacity spectrum with the corresponding damage limit states was given in Fig. 11.

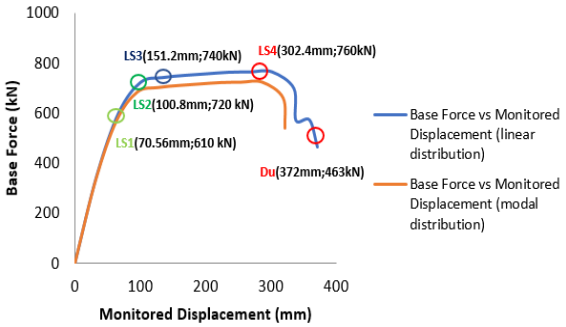

(a) Capacity curve in *x*-direction

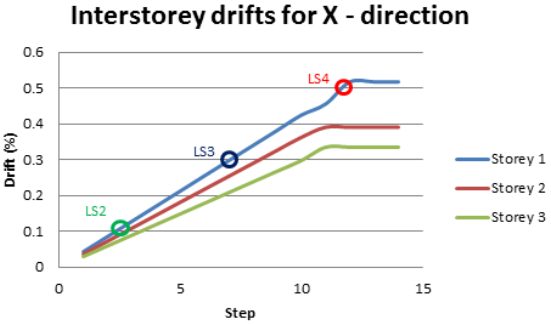

(b) Inter-storey drifts for *x*-direction

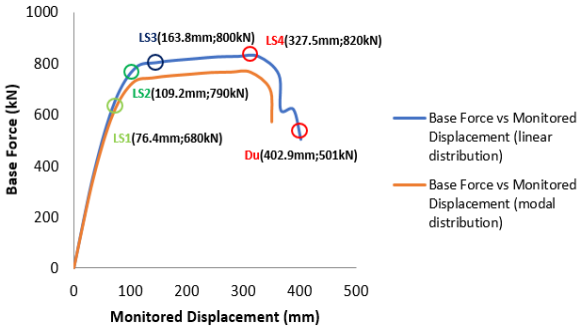

(c) Capacity curve in *y*- direction

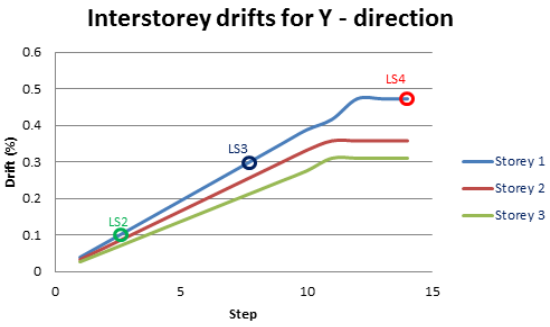

(d) Inter-storey drifts for *y* direction

Fig. 12 Capacity curves and Inter-storey drift ratios of *3*-storey URM building

According to Lagomarsino and Penna (2003), yield point and ultimate drift were firstly identified for a structure and then split the capacity curve into five parts. Damage limits separating the slight, moderate, extensive and complete regions were determined by using the outlined criteria (Table 4); the thresholds of the spectral displacements were obtained for the corresponding damage limit states.

Table 2 Modal periods, frequencies and modal participating mass ratios for 3- and 5-storey buildings

Case	Mode	3-storey building				5-storey building			
		Period	Circular Frequency	Modal Participating Mass Ratio		Period	Circular Frequency	Modal Participating Mass Ratio	
		sec	rad/sec	*Ux*	*Uy*	sec	*Ux*	*Ux*	*Uy*
Modal	1	0.235	26.725	0.876	0	0.463	13.571	0.887	0
Modal	2	0.164	38.218	0.877	0	0.323	19.448	0.888	0
Modal	3	0.137	45.778	0.877	0.898	0.270	23.281	0.888	0.909
Modal	4	0.049	128.038	0.881	0.898	0.097	65.090	0.892	0.909
Modal	5	0.048	131.382	0.983	0.898	0.095	66.447	0.995	0.909
Modal	6	0.042	149.496	0.983	0.985	0.083	75.939	0.995	0.997
Modal	7	0.024	258.125	0.983	0.985	0.047	132.893	0.995	0.997

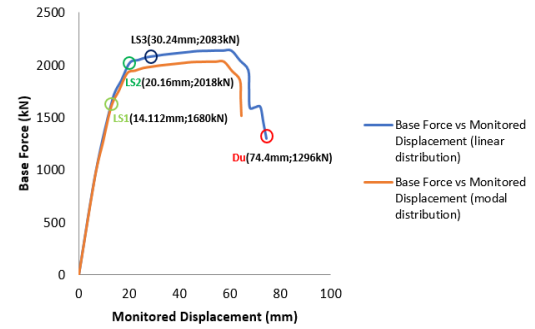

(a) Capacity curve in *x*-direction

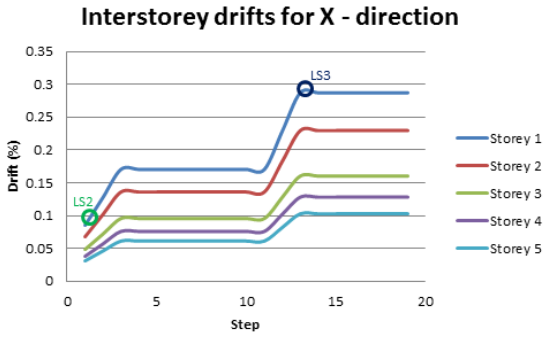

(b) Inter-storey drifts for *x*-direction

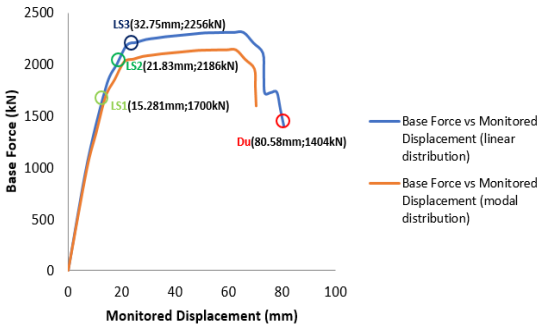

(c) Capacity curve in *y*-direction

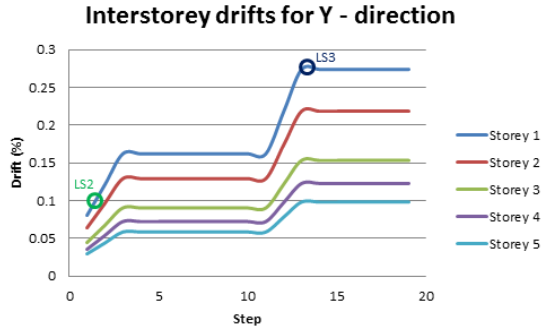

(d) Inter-storey drifts for *y*-direction

Fig. 13 Capacity curves and Inter-storey drift ratios of 5-storey Confined masonry building

5. Dynamic characteristics

The modal analysis was executed for the building models using DIANA v 9.6 and the results were presented for seven modes of vibrations. The results of the linear modal analyses were synthesized in Table 2 in terms of periods, frequencies and modal mass participating ratios.

6. Strength and deformation capacities of studied buildings

The non-linear static analysis consists of the application of gravity loads and a representative load pattern. Gravity loads were in place during lateral loading and calculated by the combination of the Dead loads and 30% of the live loads. Horizontal forces were applied monotonically in a stepwise fashion. As the loads and displacements increase, the strength and stiffness values change owing to imposed deformations. In pushover analysis, the response of the structure is presented through a capacity curve which usually gives the relation between the base shear and roof displacement.

Upon completing the aforementioned modeling procedure, the capacity curves of the buildings were determined by carrying out pushover analysis. Selection of the lateral load pattern has an imperative effect on the results. Pushover analysis with invariant load patterns have been used frequently for seismic performance evaluation in literature. One of the drawbacks of this analysis procedure is that for masonry structures so far best load pattern is not determined yet. Frequently-used load patterns are those proportional to the first mode shape, inverted triangular (Lourenço *et al*. 2012, Bilgin and Frangu 2017) and to the mass of the structure (Betti and Vignoli 2011). For the scope of the analyses, two types of lateral load distributions namely; inverted triangular and mode shapes were applied to the mass center of each storey considering the seismic

Table 3 Performance levels and criteria provided by Calvi (1999)

Performance Level	Performance Criteria
Limit State 1 (LS1)	• No damage.
Limit State 2 (LS2) (*Minor structural damage and/or moderate non-structural damage*)	• Structure can be utilized after the earthquake, without any need for significant strengthening and repair to structural elements. • The suggested drift limit is 0.1%.
Limit State 3 (LS3) *(Significant structural damage and extensive non-structural damage)*	• The building cannot be used after the earthquake without significant repair. Still, repair and strengthening is feasible. • The suggested drift limit is 0.3%.
Limit State 4 (LS 4) *(Collapse)*	• Repairing the building is neither possible nor economically reasonable. The structure will have to be demolished after the earthquake. Beyond this limit state global collapse with danger for human life has to be expected. • The suggested drift limit is 0.5%.

Table 4 Performance levels and criteria provided by Lagomarsino and Penna (2003)

Damage limit state	Spectral displacement, S_d
No damage	$S_d<0.7D_y$
Slight (SD)	$0.7D_y<S_d\leq D_y$
Moderate (MD)	$D_y<S_d\leq D_y+0.25(D_u-D_y)$
Extensive (ED)	$D_y+0.25(D_u-D_y)<S_d\leq D_u$
Complete	$S_d>D_u$

Table 5 Damage limit states of 3-Storey building according to Lagomarsino and Penna (2003)

Damage state	Spectral displacement (mm)	
	x-direction	*y*-direction
No damage	$S_d<70.6$	$S_d<76.4$
Slight	$70.6<S_d\leq100.8$	$76.4<S_d\leq109.2$
Moderate	$100.8<S_d\leq151.2$	$109.2<S_d\leq163.8$
Extensive	$151.2<S_d\leq302.4$	$163.8<S_d\leq327.5$
Complete	$S_d>302.4$	$S_d>327.5$

weight. Seismic weight of the URM buildings was calculated by considering the combination of Dead (G) and Live (Q) loads (G+0.3 Q). Consequently, damage limit states of the studied buildings were calculated and marked on capacity curves. In this study were used the damage limit states provided Lagomarsino and Penna (2003), Calvi (1999). Following the outlined criteria in Table 3-4; the thresholds of the displacements are calculated for the damage limit states. Performance levels were estimated and presented in Tables 5-6.

where;

D_y: Yield displacement;

D_u: Ultimate displacement value.

In Figs. 12-13 capacity curves and inter-storey drift plots for two types of load patterns are shown for the buildings.

Seismic capacity evaluation of the investigated buildings was performed using damage limit states by Calvi (1999).

Starting from the suggestions of Table 3, using the values of D_y and D_u obtained for both buildings from pushover analyses, damage limit states were identified (Tables 5-6).

Table 6 Damage limit states of 5-Storey building according to Lagomarsino and Penna (2003)

Damage state	Spectral displacement, S_d (mm)	
	x-direction	*y*-direction
No damage	$S_d<14.12$	$S_d<15.28$
Slight	$14.12<S_d\leq20.16$	$15.28<S_d\leq21.83$
Moderate	$20.16<S_d\leq30.24$	$21.83<S_d\leq32.75$

Table 7 Inter-storey drift distribution URM building

# of steps	*X*-Direction			*Y*-Direction		
	Storey 1	Storey 2	Storey 3	Storey 1	Storey 2	Storey 3
1	0.042	0.036	0.029	0.039	0.033	0.027
2	0.085	0.072	0.059	0.078	0.066	0.055
3	0.127	0.108	0.089	0.116	0.099	0.082
4	0.169	0.145	0.119	0.155	0.133	0.109
5	0.212	0.181	0.149	0.194	0.165	0.137
6	0.254	0.217	0.179	0.233	0.199	0.165
7	0.296	0.253	0.209	0.272	0.232	0.192
8	0.339	0.289	0.239	0.310	0.265	0.219
9	0.381	0.325	0.269	0.349	0.298	0.247
10	0.423	0.362	0.299	0.388	0.332	0.275
11	0.454	0.389	0.336	0.417	0.357	0.309
12	0.516	0.389	0.336	0.473	0.357	0. 309
13	0.516	0.389	0.336	0.473	0.357	0. 309
14	0.516	0.389	0.336	0.473	0.357	0. 309

On the other hand, the correct prediction of inter-storey drift ratio and its distribution along the height of the buildings is imperative for the earthquake performance assessment purposes since the structural damage is directly associated with this parameter. The inter-storey drift ratios and their distribution along the height of the buildings were given in Tables 7-8 and plotted in Figs. 12-13(b), (d). Distribution of the inter-storey ratio over the height of 3-storey building is uniform, whereas this distribution is non-uniform for 5-storey building as wall thickness suddenly reduces at the third storey (Figs. 13(b), (d)).

7. Estimation of seismic demand

Earthquake loads are usually represented by response spectrum functions which are derived from time history records of past earthquakes in specific locations. In order to perform a reliable seismic performance assessment, seismic demands of the studied buildings were determined based on detailed seismic hazard assessment. A detailed soil investigation was carried out in order to have a comprehensive understanding of the actual structural conditions for Lapraka area where both buildings are located. The boreholes were drilled, and the samples were analyzed. A seismic hazard assessment for Lapraka area was carried out (Aliaj *et al*. 2014). The peak ground acceleration (PGA) was calculated for stiff soil conditions

Table 8 Inter-storey drift distribution 5-storey building

# of steps	*X*-Direction					*Y*-Direction				
	Storey 1	Storey 2	Storey 3	Storey 4	Storey 5	Storey 1	Storey 2	Storey 3	Storey 4	Storey 5
1	0.085	0.068	0.048	0.038	0.030	0.081	0.065	0.045	0.036	0.029
2	0.128	0.102	0.072	0.057	0.0459	0.122	0.097	0.068	0.055	0.044
3	0.171	0.137	0.096	0.077	0.0612	0.162	0.129	0.091	0.073	0.058
4	0.171	0.137	0.056	0. 077	0. 0612	0.162	0.129	0.091	0.073	0.058
5	0.171	0.137	0.056	0. 077	0. 0612	0.162	0.129	0.091	0.073	0.058
6	0.171	0.137	0.056	0. 077	0. 0612	0.162	0.129	0.091	0.073	0.058
7	0.171	0.137	0.056	0. 077	0. 0612	0.162	0.197	0.091	0.073	0.058
8	0.171	0.137	0.056	0. 077	0. 0612	0.162	0.129	0.091	0.073	0.058
9	0.171	0.137	0.056	0. 077	0. 0612	0.162	0.129	0.091	0.073	0.058
10	0.171	0.137	0.056	0. 077	0. 0612	0.162	0.129	0.091	0.073	0.058
11	0.171	0.137	0.056	0. 077	0. 0612	0.162	0.129	0.091	0.073	0.058
12	0.229	0.183	0.123	0.103	0.0821	0.218	0.174	0.122	0.097	0.078
13	0.288	0.230	0.161	0.189	0.1031	0.273	0.219	0.153	0.122	0.098
14	0.288	0.230	0.161	0. 189	0.1031	0.273	0.219	0.153	0.122	0.098
15	0.288	0.230	0. 161	0. 189	0. 1031	0.273	0.219	0.153	0.122	0.098
16	0.288	0.230	0. 1611	0. 189	0. 1031	0.273	0.219	0.153	0.122	0.098
17	0.288	0.230	0. 161	0. 189	0. 1031	0.273	0.219	0.153	0.122	0.098
18	0.288	0.230	0. 161	0. 189	0. 1031	0.232	0.219	0.153	0.122	0.098
19	0.288	0.230	0.1611	0. 189	0. 1031	0.273	0.219	0.153	0.122	0.098

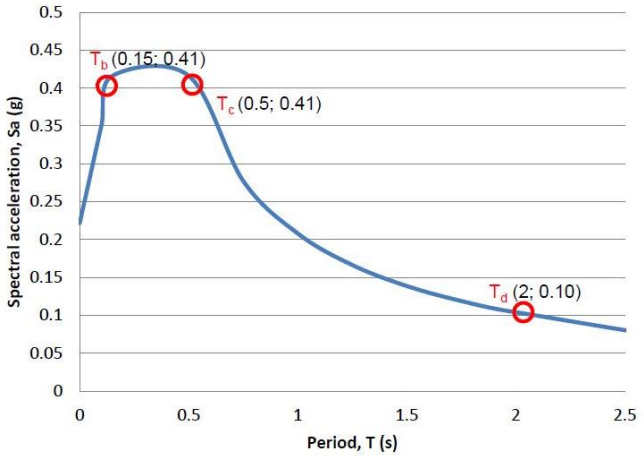

Fig. 14 Elastic acceleration response spectrum

with an estimation of 0.248 g. In this study, the demand calculations for the seismic assessment of the considered buildings were performed considering the actual soil conditions with a moderate seismicity (~0.25 g) according to Eurocode 8. Seismic demand spectra used in performance assessment was given in Fig. 14 where corner periods are represented by T_b, T_c and T_d.

Nonlinear displacement demands could be estimated based upon *R*-μ-*T* based demand approaches (Fajfar and Zamfirescu 2001) like N2 method in Eurocode 8 or damping based studies namely capacity spectrum methods proposed by several researchers (Freeman *et al.* 1975) adopted by several international guidelines (ATC-40 and ATC-2005). In this study, two approaches adopted by EC8 and FEMA 440 guidelines were used. By this way, effects of two different demand calculations on seismic performance evaluation of masonry buildings were compared. In each approach, earthquake demands were estimated using equal displacement approach (ESDOF). Multi degree of freedom system (MDOF) was transformed to SDOF systems by a single constant and modal participation factor. Determination of seismic demand according to EC8 is stated as follows:

1. Determine the seismic demand for the site in the shape of elastic spectrum. Spectral acceleration is given with respect to period.
2. Determine the target displacement with the following relationship

$$S_{de} = S_{ae}\omega^2 = S_{ae}\frac{T^2}{4\pi^2} \tag{5}$$

$$S_a = \frac{S_{ae}}{R_\mu} \tag{6}$$

$$S_d = S_a\mu\frac{T^2}{4\pi^2} \tag{7}$$

1. Apply lateral forces to non-linear modal and construct pushover curve, idealize as a bilinear capacity curve,
2. Modify capacity curve to a capacity spectrum in ADRS format.
3. Determine location of intersection point. If in inelastic range, develop inelastic demand spectrum. Calculate SDOF spectral displacement demand and convert to MDOF displacement demand.

On the other hand, Capacity spectrum method provides another approach to estimate the seismic demands. Seismic demands are calculated by considering inelastic response of the building which is simulated by capacity curves. In this method, capacity curve and demand spectrum should be transformed to ADRS. Bilinear or trilinear representation of capacity curve is required like in EC8. Then, an initial performance point is selected as defined in FEMA 440. By using the values obtained from the bilinear representation

Table 9 Earthquake demand values calculated according to FEMA-440 and EC 8

	Direction	Comparison of Performance points according to FEMA-440 and EC8			
		3- Storey building		5- Storey building	
		Sa (g)	S_d (mm)	*Sa* (g)	S_d (mm)
Eurocode 8	*x*	0.15	148	0.39	51.0
	y	0.15	147	0.41	47.1
FEMA-440	*x*	0.12	174	0.35	61.0
	y	0.13	157	0.36	59.5

capacity spectrum, post elastic stiffness and ductility factors were calculated to determine the effective damping and the corresponding effective period. Using the effective damping, ordinates of the spectral acceleration can be adjusted. Estimated target displacement is determined by using the intersection of effective period and ADRS adjusted for effective damping. The estimated maximum acceleration corresponds to the target displacement on the pushover curve. Finally, these obtained values are transformed to roof displacement and base shear by using Eqs. (8) and (9).

$$V_T = \alpha_1 S_a \tag{8}$$

$$\delta_{max} = PF_1 \emptyset_{roof} S_d \tag{9}$$

where;

S_{de}-S_{de} : Values from elastic spectrum (displacement and acceleration) for period T and corresponding damping,
μ : Ductility factor,
T : Period,
R_μ : Reduction factor,
S_d -S_a : Spectral displacement - acceleration,
V_T : Total base shear,
α_1 : Modal mass coefficient for the first natural mode,
PF_1 : Modal participation factor for the first natural mode,
$\delta_{\max}$: Maximum roof displacement,

8. Performance evaluation of masonry buildings

The displacement capacity values are merely not meaningful themselves. They need to be compared with demand values. Seismic demands of both buildings in both directions were calculated by using EC-8 and FEMA-440 guidelines. According to many modern guidelines, residential buildings are expected to meet "Life Safety" performance level which corresponds to LS3 according to Calvi (1999) under design earthquakes, corresponding to 10% probability of exceedance in 50 years.

Earthquake demand estimates and damage limit states of building capacities corresponding to calculated performance levels were compared to see whether the residential buildings have adequate capacity (Figs. 15-18). Table 9 lists performance points (PP) levels of each building according to EC-8 and FEMA-440 (Figs. 15-18.).

From the comparison of the calculated damage limit states (Table 5) and the demand estimates (Table 9), 3-storey buildings was expected to experience extensive damage (Table 10).

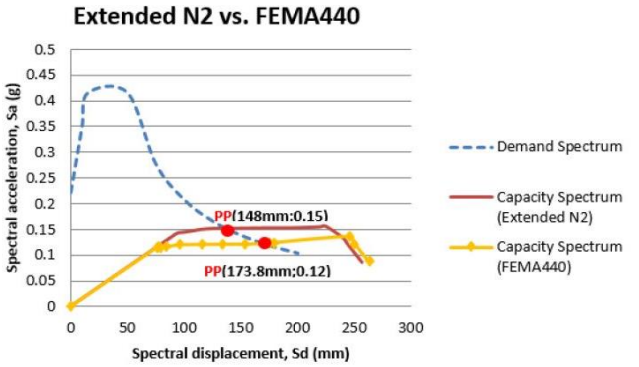

Fig. 15 Comparison of N2 and FEMA 440 methodologies for 3-storey building (*x*-direction)

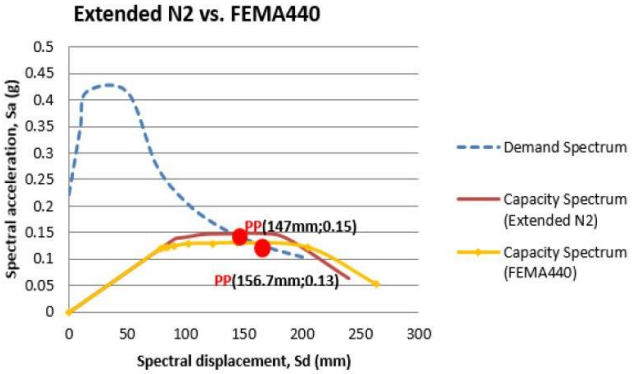

Fig. 16 Comparison of N2 and FEMA 440 methodologies for 3-storey building (*y*-direction)

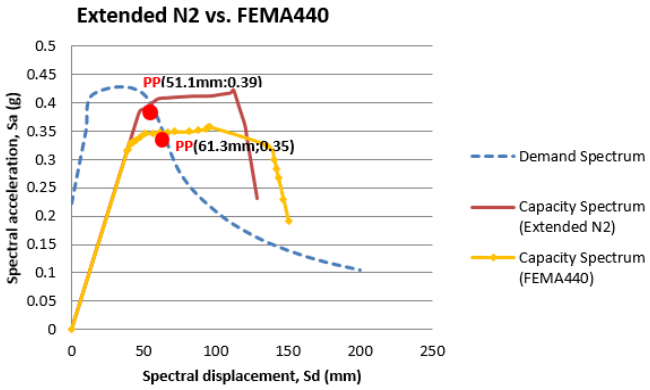

Fig. 17 Comparison of N2 and FEMA 440 methodologies for 5-storey building (*x*-direction)

Table 10 Damage limit states for 3- storey building (Lagomarsino and Penna 2003)

Damage limit states	*x*-direction	*y*-direction
	Spectral displacement, S_d	
No damage	S_d<55.5	S_d<59.22
Slight	55.5<S_d≤79.28	59.22<S_d≤84.6
Moderate	79.28<S_d≤120.91	84.6<S_d≤114.8
Extensive	120.91<S_d≤245.8	114.8<S_d≤205.2
Complete	S_d>245.8	S_d>205.2

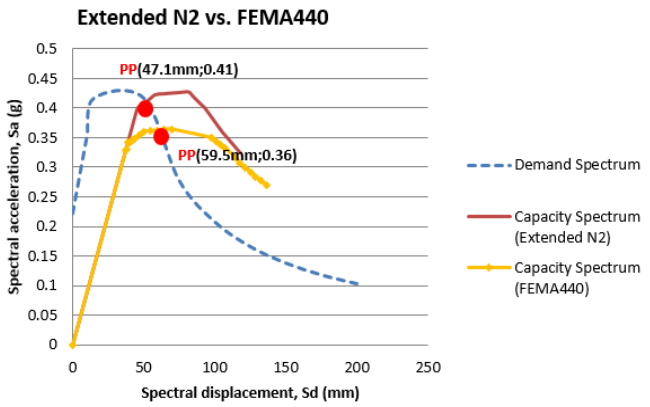

Fig. 18 Comparison of N2 and FEMA 440 methodologies for 5-storey building (*y*-direction)

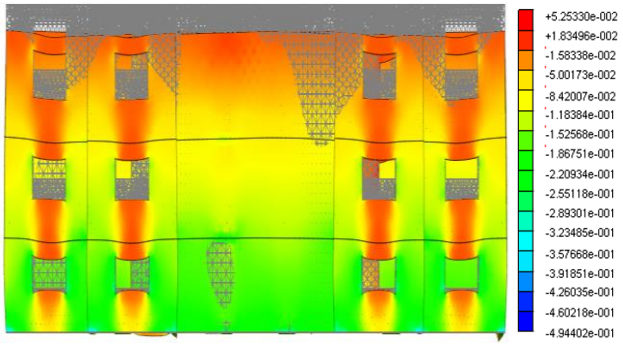

Fig. 19 Shear stress distribution in LS4 stage for façade wall element obtained from pushover analysis in *x*-direction for 3-storey building - (MPa)

Table 11 Damage Limit states for 5-storey building (Lagomarsino and Penna 2003)

Damage limit states	*x*-direction	*y*-direction
	Spectral displacement, S_d	
No damage	S_d<28.3	S_d<27.4
Slight	28.3<S_d≤40.4	27.4<S_d≤39.2
Moderate	40.4<S_d≤64.3	39.2<S_d≤60.6
Extensive	64.3<S_d≤135.8	60.6<S_d≤124.9
Complete	S_d>135.8	S_d>124.9

From the comparison of the calculated damage limit states (Table 6) and the demand estimates (Table 9), 5-storey buildings was expected to experience moderate damage (Table 11).

Performance assessment results were summarized in Table 12.

9. Remarks on building responses

For 3- storey building in *x*-direction; the linear distribution of seismic loads shows a more ductile behavior of the structure than the modal one. Although the results state a ductile behavior of the structure, the appearance of LS4 indicates an extensive damage state. From the distribution of shear stress at LS4 stage, it is noticed that spandrel elements fail, although most of masonry does not reach ultimate shear resistance (Fig. 19). As seen from the distribution of inter-storey drifts (Fig. 12) the drift limit is at 0.5%. According to damage classification by Calvi (1999), repairing the building is neither possible nor economically reasonable. Beyond this limit state, global collapse with danger for human life could be expected.

Like in the *x*- direction, the linear distribution shows a more ductile behavior in *y*- direction. Even in this direction the appearance of LS4 indicates an extensive damage state. A reason for this similarity is the symmetrical distribution of the load bearing walls in both directions. Both guidelines state that the structure shows low stiffness in *x*- direction. Although FEMA440 reveals that load bearing walls are still in function, the damages are significantly high and the serious risk to collapse is present. The poor seismic performance is confirmed for the *y*- direction by the position of the performance point which stands between LS3 and LS4 for both spectrums. Both codes indicate low stiffness in *y*- direction with a high risk of collapse. Intervention to improve the seismic capacity of the building seems not economically reasonable.

For 5- storey building; capacity curves (Fig. 13) show a ductile response of the structure in *x*- direction. Unlike the

Table 12 Comparison of damage states and performance levels

Building Type	Direction	Performance levels		Comments	
		EC-8	FEMA-440	Damage State	Performance levels
3- Storey	*x*	Risky*	Collapse Prevention Level	Low stiffness. Performance is close to collapse	Little residual stiffness and strength, but load bearing walls function. Building is near collapse.
	y	Risky*	Collapse Prevention Level	Low stiffness. Performance is close to collapse	Little residual stiffness and strength, but load bearing walls function. Building is near collapse.
5- Storey	*x*	Safe LS3	Life Safety Level	Moderate damage	Moderate damage. Some residual strength and stiffness left in all stories. Gravity load bearing elements function. Somewhat more damage and slightly higher risk.
	y	Safe LS3	Life Safety Level	Moderate damage	Moderate damage. Some residual strength and stiffness left in all stories. Gravity load bearing elements function. Somewhat more damage and slightly higher risk.

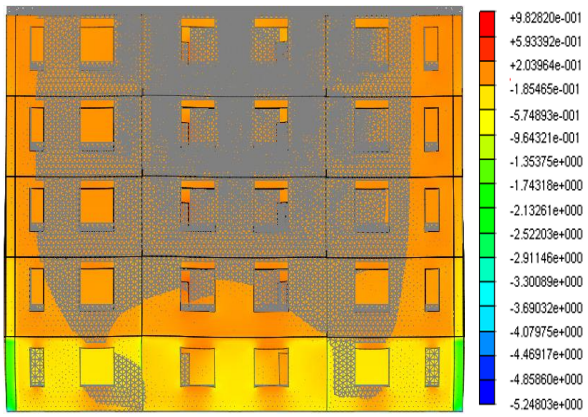

Fig. 20 Shear stress distribution in the maximum base shear point obtained from pushover analysis in *x*- direction for 5-storey building - (MPa)

URM case study building, the LS4 performance stage does not appear. This means that none of the elements (spandrels and piers) fails until the masonry reaches the ultimate shear resistance (Fig. 20).

As can be seen from Fig. 13 the drift limit does not exceed 0.3%. According to damage classification by Calvi (1999), the structure has significant structural damage and extensive non-structural damage. The repair and strengthening of the structure is considered to be feasible. A "jump", which is a sudden and drastic change in the inter-storey drift percentage is noticed in the graphs. This is due to thickness reduction of the outer load bearing walls (from 380 mm to 250 mm), starting from the third storey. The results obtained from the analysis in *y*- direction confirm the performance of the confined masonry case study building previously determined for the *x*- direction.

The tendency of FEMA440 to indicate a more ductile behavior is confirmed for this case study building too. The presence of tie elements such as bond beams and tie columns, affects positively the seismic resistance of the structure. This is noticed where these tie elements show a considerable stress value. Another reason for the higher performance is the material properties of the masonry units. The load bearing walls at the first two stories of the confined masonry building (380mm) are considerably thicker than the ones in the URM building (250mm), which favorably affects the structural performance by increasing stiffness.

10. Conclusions

This paper has presented the seismic performance evaluation of two typical masonry buildings which represent the low and mid-rise residential building stock in Albania. Three dimensional structural models were simulated, and general properties of the members were determined based on experimental tests. The seismic capacities of the buildings were estimated by using a structural model which uses macro modeling approach for the load bearing masonry walls using DIANA v 9.6.

Capacity curves were obtained by pushover analyses. The seismic demand has been estimated according to EC 8 and FEMA 440 guidelines. Two types of damage limit states were used by Calvi (1999), Lagomarsino and Penna (2003) to specify the seismic performance. The findings of the study can be stated as follows:

- Based on the test results, the URM building was made of solid bricks with 18.06 MPa compressive strength and mortar with 3.88 MPa, while the Confined Masonry was made of calcium silicate solid bricks with 16.52 MPa compressive strength and the mortar with 10 MPa.
- Evaluation of the capacity curves demonstrated that URM building performs poor. The presence of LS4 performance stage indicates an extensive damage according to Lagomarsino and Penna (2003). Most of spandrel elements fail before the structure reaches the ultimate limit state under horizontal seismic loads. Confined Masonry building performed better. According to the above-mentioned classification, damage state is considered to be moderate.
- Capacity curves highlight the influence of the lateral load pattern on building response. The linear distribution shows a more ductile behaviour than the modal one. It does also show a greater base shear demand compared to the modal one.
- Interstorey drifts are limited to 0.5% for the URM case study. According to damage classification by Calvi (1999), repairing the building is neither possible nor economically reasonable. The drift limit is reduced to 0.3% for the confined masonry building which means that the structure has significant structural damage and extensive non-structural damage but still, repair and strengthening might be feasible.
- Regarding the distribution of inter-storey drift and stress distribution for 5- storey building, due to the sudden reduction of wall thickness from second to third storey, stress and drift concentration are accumulated at this level. Such abrupt changes in thickness of load bearing walls on masonry buildings can cause serious damages in this type of structures. Distribution of the wall thickness over the height of the building should be uniform or gradually changing to prevent this type of inconvenience.
- Since these masonry buildings were designed according to the forced based design philosophy, such aforementioned deficiencies (wall thickness change) may not be determined by force-based evaluation procedures. On the other hand, displacement-based methods are believed to be useful tools to capture such deficiencies in this type of masonry construction.
- According to N2 method, the performance of URM building was found to be "Risky", with low stiffness and severe damages of structural components for both directions. The Capacity Spectrum Method (FEMA 440) confirms the low stiffness and severe damages by indicating the "Collapse Prevention" performance level. The seismic performance of the confined masonry building is evaluated as "Safe" according to N2 method and "Life Safety" performance level according to FEMA440.
- The past earthquake damages on URM buildings support the analytical results of this study. Recent

studies (Kaplan *et al*. 2010, Klingner 2006) from past earthquakes pointed out masonry facades with various spandrels and between those spandrels failed due to shear. Shear stress concentrations on spandrels observed in pushover analyses for these buildings are clear indicators of such failures and potential risk in existing masonry buildings.

In the light of this analysis results, it can be stated that decision makers should be aware of the catastrophic nature of such brittle systems when weighing options for earthquake mitigation because a large inventory of the existing structures is composed of masonry and constructed prior to legislation of new guidelines.

References

Aliaj, S. and Allkja, S. (2014), "Studim inxhiniero-sizmologjik i sheshit te ndertimit te objektit me laretsi 2-7 kate me 1 kat nentoke ne rrugen 'Don Bosko'", *Ne zonen e Laprakes*, Tirana, Albania.

American Association State Highway and Transportation Officials Standard, Designation: C67-09 (2008), Standard Test Methods for Sampling and Testing Brick and Structural Clay Tile.

Augenti, N. and Paris, F. (2011), "Constitutive modeling of tuff masonry in direct shear", *Constr. Build. Mater.*, **25**(4), 1612-1620.

Benedetti, D., Carydis, G. and Pezzoli, P. (1998), "Shaking table tests on 24 simple masonry buildings", *Earthq. Eng. Struct. Dyn.*, **27**(1), 67-90.

Betti, M. and Vignoli, A. (2011) "Numerical assessment of the static and seismic behavior of the basilica of Santa Maria all'Impruneta (Italy)", *Constr. Build. Mater.*, **25**(12), 4308-4324.

Bilgin, H. (2007), "Seismic performance evaluation of public buildings using non-linear analysis procedures and solution methods", Pamukkale University, Denizli, Turkey.

Bilgin, H. (2013), "Fragility-based assessment of public buildings in Turkey", *Eng. Struct.*, **56**, 1283-1294.

Bilgin, H. (2015), "Generation of fragility curves for typical RC health care facilities: Emphasis on hospitals in Turkey", *J. Perform. Constr. Facil.*, **30**(3), 04015056.

Bilgin, H**.** and Frangu, I. (2017), "Predicting the seismic performance of typical R/C healthcare facilities: emphasis on hospitals", *Int. J. Adv. Struct. Eng.*, **9**(3), 277-292.

Bilgin, H. and Huta, E. (2016), "Earthquake performance assessment of low-rise URM building", *Proceedings of the 3rd International Balkans Conference on Challenges of Civil Engineering*, Epoka University, Tirana, May.

Bilgin, H. and Korini, O. (2012), "Seismic capacity evaluation of unreinforced masonry residential buildings in Albania", *Nat. Hazard. Earth Syst. Sci.*, **12**(12), 3753-3764.

Cagnan, Z. (2012), "Numerical models for the seismic assessment of St. Nicholas Cathedral, Cyprus", *Int. J. Soil Dyn. Earthq. Eng.*, **39**, 50-60.

Calderini, C. and Lagomarsino, S. (2008), "A continuum model for in-plane anisotropic inelastic behaviour of masonry", *J. Struct. Eng.*, ASCE, **134**(2), 209-220.

Calvi, G.M. (1999), "A displacement-based approach for vulnerability evaluation of classes of buildings", *J. Earthq. Eng.*, **3**(3), 411-438.

Chen, S.Y., Moon, F.L. and Yi, T. (2008), "A macroelement for the nonlinear analysis of in-plane unreinforced masonry piers", *Eng. Struct.*, **30**, 2242-2252.

Decanni, L., D'Amore, E., Goretti, A., Langenbach, R., Mollaioli, F. and Rasulo, A. (2004), "Performance of masonry buildings during the 2002 Molise, Italy earthquake", *Earthq. Spectra*, **20**, 191-220.

DIANA (2014), Finite Element Analysis: User's Manual, Concrete and Masonry Analysis, Netherlands.

EN 1998-1 (2004), Eurocode 8: Design of Structures for Earthquake Resistance - Part 1: General Rules, Seismic Actions and Rules for Buildings, The European Union Per Regulation 305/2011, Directive 98/34/EC, Directive 2004/18/EC.

Eurocode 6 (1996), Design of Masonry Structures - Part 1-1: General Rules for Buildings-Rules for Reinforced and Unreinforced Masonry, European Committee for Standardization, Brussels.

Farshchi, D.M., Motavall, M., Schumacher, A. and Marefat, M.S. (2009), "Numerical modeling of in-plane behaviour of URM walls and an investigation into the aspect ratio, vertical and horizontal post-tensioning and head joint as a parametric study", *Arch. Civil Mech. Eng.*, **9**(1), 5-27

Fema-440 (2005), "Improvement of nonlinear static seismic analysis procedures", Applied Tech. Council.

Foraboschi, P. and Vanin, A. (2013a), "Non-linear static analysis of masonry buildings based on a strut-and-tie modeling", *Soil Dyn. Earthq. Eng.*, **55**, 44-58.

Freeman, S.A., Nicoletti, J.P. and Tyrell, J.V. (1975), "Evaluations of existing buildings for seismic risk-A case study of Puget sound naval shipyard, Bremerton, Washington", *Proceedings of U.S. National Conference on Earthquake Engineering*, Ann Arbor, Michigan, June.

Huta, E. (2015), "Earthquake performance assessment of a low- and mid-rise URM building", MSc Thesis, Epoka University, Tirana, Albania.

Inel, M., Bilgin, H. and Ozmen, H.B. (2008), "Seismic capacity evaluation of school buildings in Turkey", *Pro. Inst. Civil Eng., Struct. Build.*, **161**(3), 147-159.

Kaplan, H., Bilgin, H., Yilmaz, S., Binici, H. and Oztas, A. (2010), "Structural damages of L'Aquila earthquake", *Nat. Hazard. Earth. Syst. Sci.*, **10**, 499-507.

Klingner, R.E. (2006), "Behavior of masonry in the Northridge (US) and Tecoma´n-Colima (Mexico) earthquakes: Lessons learned, and changes in US design provisions", *Constr. Build. Mater.*, **20**, 209-19.

Korini, O. (2012), "Seismic assessment of albanian masonry buildings using nonlinear procedures", MSc Thesis, EPOKA University, Tirana, Albania.

Korkmaz, K.A. (2009), "Seismic safety assessment of unreinforced masonry low-rise buildings in Pakistan and its neighborhood", *Nat. Hazard. Earth Syst. Sci.*, **9**(3), 1021-1031.

KTP-9-78 (1978), Albanian Masonry Design Code, Tirana, Albania.

KTP-N2-89 (1989), Albanian Seismic Design Code, Tirana, Albania.

Lagomarsino, S. and Penna, A. (2003), "Guidelines for the implementation of the II level vulnerability methodology. WP4: Vulnerability assessment of current buildings. RISK-UE project: An advanced approach to earthquake risk scenarios with application to different European towns", Contract Number EVK4-CT-2000-00014.

Lagomarsino, S., Galasco, A. and Penna, A. (2007), "Nonlinear macro element dynamic analysis of masonry buildings", *Proceedings of the ECCOMAS Thematic Conference on Computational Methods in Structural Dynamics and Earthquake Engineering*, Rethymno, Crete.

Lourenço, P.B. (1996), "Computational strategies for masonry structures", PhD Dissertation, Delft: Delft University Press, Netherland.

Lourenço, P.B. *Recent Advances in Masonry Modeling: Micro-Modeling and Homogenization, Multscale Modeling in Solid*

Mechanics: Computational Approaches, Eds. Ugo Galvanetto and M H Aliabadi, Imperial College Press., London.

Lourenço, P.B., Almeida, J.C. and Barros, J.A. (2005), "Experimental investigation of brick under uniaxial tensile testing", *Masonry Int.*, **18**(1), 11-20..

Lourenço, P.B., Rots, J.G. and Blaauwendraad, J. (2008), "Continuum model for masonry: Parameter estimation and validation", *J. Struct. Eng*., **124**, 642-652.

Lourenço, P.B., Trujillo, A., Mendes, N. and Ramos, L.F. (2012), "Seismic performance of the St. George of the Latins church: Lessons learned from studying masonry ruins", *Eng. Struct.*, **40**, 501-518.

Mendes, N. and Lourenço, P.B. (2010), "Seismic assessment of masonry "Gaiolerio" buildings in Lisbon", *J. Eartq. Eng*., **14**(1), 80-101.

Preciado, A., Lester, J., Ingham, J.M., Pender, M. and Wang, G. (2014), "Performance of the Christchurch, New Zealand Cathedral during the M7.1 2010 Canterbury earthquake", *Proceedings of the 9th International Conference on Structural Analysis of Historical Constructions (SAHC*), Mexico City, October.

Preciado, A., Orduña, A., Bartoli, G. and Budelmann, H. (2015), "Façade seismic failure simulation of an old Cathedral in Colima, Mexico by 3D limit analysis and nonlinear finite element method", *J. Eng. Fail. Anal.*, **49**, 20-30.

Preciado, A., Ramirez-Gaytan, A., Gutierrez, N., Vargas, D., Falcon, J.M. and Ochoa, G. (2018), "Nonlinear earthquake capacity of slender old masonry structures prestressed with steel, FRP and NiTi SMA tendons", *Steel Compos. Struct.*, **26**(2), 213-226.

Preciado, A., Ramirez-Gaytan, A., Salido-Ruiz, R.A., Caro-Becerra, J.L. and Lujan-Godinez, R. (2015), "Earthquake risk assessment methods of unreinforced masonry structures: Hazard and vulnerability", *Eartq. Struct.*, **9(**4), 719-733.

Preciado, A., Sperbeck, S.T. and Ramirez-Gaytan, A. (2016), "Seismic vulnerability enhancement of medieval and masonry bell towers externally prestressed with unbonded smart tendons", *J. Eng. Struct.*, **122**, 50-61.

Taylor, R.L. and Zhu, J.Z. (2005), *The Finite Element Method: its Basis and Fundementals*, Elsevier.

Wang, S.Y., Sloan, S.W., Abbo, A.J., Masia, M.J. and Tan, C.A. (2012), "Numerical simulation of the failure process of unreinforced masonry walls due to concentrated static and dynamic loading", *Int. J. Solid. Struct.*, **49**(2), 377-394.

Yılmaz, S., Tama, Y.S. and Bilgin, H. (2013), "Seismic performance evaluation of unreinforced masonry school buildings in Turkey", *J. Vib. Control*, **19**(16), 2421-2433.

Zamfirescu, D. and Fajfar, P. (2001), "Comparison of simplified procedures for nonlinear seismic analysis of structures", *The Third U.S.-Japan Workshop on Performance-Based Earthquake Engineering Methodology for Reinforced Concrete Building Structures*, Seattle, Washington, August.

CC